Forbidden (222) Neutron Reflection in Silicon: Anharmonicity and the Bonding Electrons†

David Keating and Anthony Nunes
Brookhaven National Laboratory, Upton, New York 11973

and

Boris Batterman and Jerome Hastings
Department of Materials Science and Engineering, Cornell University, Ithaca, New York 14850

(Received 22 June 1971)

Using neutrons, the "forbidden" (222) reflection in silicon was detected and measured between 15 and 1353 °C. At 1001 °C the Dawson and Willis anharmonic-force constant was evaluated as $\beta = 2.99\times10^{-12}$ ergs/Å^3 which is close to that derived from the thermal expansion of silicon. We have used these neutron measurements to correct the x-ray (222) structure factor for the anharmonic atomic motion. The scattering from the anticentrosymmetric valence-charge density obtained in this way is found to be less temperature dependent than that from the core electrons. We take this as evidence in support of the shell model and of the failure of the rigid ion model.

I. INTRODUCTION

Silicon has the diamond structure which can be visualized as two fcc lattices separated by $\frac{1}{4}$ of the cube diagonal. We may distinguish the two fcc lattices by denoting them A and B. The sites of these two lattices both have T_D point symmetry, but the sites on the B lattice differ from those in the A lattice by inversion symmetry. The nearest neighbors of an A site all lie on the B lattice and vice versa. For quadricovalent silicon, tetrahedral orientation of bonds is expected with $3s$-$3p$ hybridization.[1] The tetrahedral hybrid from the A site is able to overlap strongly with the oppositely directed hybrid of the B site giving strong bonding and a net charge density that is anticentrosymmetric with respect to either site. Those reflections with Miller indices such that $h+k+l=$ (Modulo 4)$+2$ are the so called "forbidden" reflections and have a structure factor $F(h,k,l)=4(f_A-f_B)$. The f's are the Fourier transform of the time-averaged charge density of the two sites. Thus, the intensity of this class of reflections is a direct measure of the anticentrosymmetric charge density of the two sites. This has long been recognized as the explanation for the otherwise forbidden reflections observed in diamond structures.[2] A recent x-ray measurement[3] gives $F(2,2,2)=1.46\pm0.04$ for silicon.

However, another possible cause for site asymmetry can exist in diamond structures. Because of their tetrahedral environment, each atom sees a nearest neighbor in one direction and a "hole" in the opposite direction. At high temperatures, we might anticipate that an atom spends more of its time making excursions toward the hole than toward its neighbor. This anharmonicity in atomic motions would create a time-averaged asymmetry, also tetrahedral, in the nuclear distribution. When considered together, anharmonic motion of the core charge and bonding charge work against each other in the sense that the time-averaged charge distribution becomes more spherical. These combined effects become difficult to sort out using x rays alone.[3] However, neutrons, interacting with what. for all practical purposes, is a point nucleus measure only the time-averaged anticentrosymmetric nuclear distribution of the two sites resulting from anharmonic thermal motion. Thus, by combining x-ray and neutron measurements these two effects can be sorted out.

Dawson and Willis[4] have formulated the problem for the motion of the atoms in terms of an effective Einstein potential of the form

$$V_A(\vec{r}) = V_0 + \tfrac{1}{2}\alpha\,(x^2+y^2+z^2) + \beta xyz$$

which satisfies the T_d site symmetry. Assuming Boltzmann statistics, they expressed the nuclear distribution as $P_A(\vec{r}) = N\,e^{-V(\vec{r})/kT}$, where N is the normalization constant, k the Boltzmann factor, and T the absolute temperature. The harmonic-force constant is α and the anharmonic-force constant is β. The potential for the B site $V_B(\vec{r})$ differs from $V_A(\vec{r})$ by a change in the sign of the anharmonic term. They express the neutron structure factor for the forbidden reflections as

$$F(h,k,l) = -8ibe^{-M}\,Y(h,k,l)\,, \tag{1}$$

where

$$Y(h,k,l) = (2\pi/\alpha)^2\,(\beta/\alpha^3)\,(hkl)\,(kT)^2\,. \tag{2}$$

Here, b is the neutron-scattering length, M the Debye-Waller factor, and a the lattice constant. They also relate M to α by

$$M = 2\pi^2 k T (h^2 + k^2 + l^2)/(\alpha a^2).$$

The thermal-expansion coefficient is given by $\chi = 8k\beta/(3\alpha^2 a)$. This expression is just twice that quoted by Dawson and Willis for fluorite in which there is only one tetrahedral site. In a diamond structure where both A and B sites are tetrahedral, a factor of 2 is required.

Aside from the dominant nuclear force interaction between the neutron and the atomic nucleus, there is a weak neutron-electron interaction first pointed out by Foldy.[5] Krohn and Ringo[6] give the value $C_f = (-1.34 \pm 0.03) \times 10^{-16}$ cm/electron for the scattering length arising from this interaction. There is also a weak interaction accompanying the neutron's close passage by a nucleus, between the neutron's magnetic moment and the strong electric fields within the atom. This Schwinger interaction[7] has been assigned[8] a scattering length $\pm iC_s(Z-f) \times \cot\theta$, where $C_s = 2.92 \times 10^{-16}$ cm, Z is the atomic number, f is the x-ray atomic form factor, and θ is is half the scattering angle. The sign depends on the orientation of the neutron spin. When these small effects are included, Eq. (1) is replaced by

$$F(h,k,l) = (A+B) + i(C+D), \tag{3}$$

where the real part depends upon neutron polarization (when an unpolarized beam is used, as in our case, the sign of this part is immaterial) and

$$\begin{aligned} A &= 8e^{-M} C_s f_b \cot\theta, \\ B &= 8e^{-M} C_s (Z - f_c) Y(h,k,l) \cot\theta, \\ C &= 8e^{-M} C_f f_b, \\ D &= 8e^{-M} (b + C_f f_c) Y(h,k,l). \end{aligned} \tag{4}$$

Here, f_b is that part of the form factor arising from the anticentrosymmetric part of the electron charge density (~ bonding electrons), and f_c is that part arising from the centrosymmetric part of the charge density (~ core electrons). The first term in D is the (222) nuclear anharmonic contribution which is the effect sought. It follows that $f_b(h,k,l) = -f_b(\bar{h},\bar{k},\bar{l})$. We have assigned a value to f_b equal to $\frac{1}{8}$ of the x-ray (222) structure factor,[3] and taken the usual silicon form factor[9] equal to 8.04 for f_c. The values assigned the other quantities[3,10,11] are $a = 5.431$ Å, $\alpha = 7.85 \times 10^{-12}$ erg Å^{-2}, and $b = 0.4151 \times 10^{-12}$ cm. For $\beta = 3.0 \times 10^{-12}$ erg Å^{-3}, $\theta = 50.0°$, and $T = 288$ °K; $A = 3.32 \times 10^{-16}$ cm, $B = 0.013 \times 10^{-16}$ cm, $C = -1.819 \times 10^{-16}$ cm, and $D = -3.74 \times 10^{-16}$ cm. At higher temperatures, the anharmonic D term predominates.

II. EXPERIMENT AND RESULTS

The anharmonic effect is small, and has been unsuccessfully sought previously.[4,12,13] In the present experiment, great care was taken to eliminate harmonics in the incident beam and possible multiple Bragg events in the sample which would mask the anharmonic (222). To make maximum use of the intense neutron flux provided by the Brookhaven High Flux Beam Reactor, a large volume single crystal of silicon was employed.

Our incident beam flux was 1.93×10^5 neutrons cm^{-2} sec^{-1}, and for the purpose of making relative measurements of the (222) reflection, a beam area of 5.54 cm^2 was used. The peak-to-background ratio of these relative measurements was optimized with 20′ horizontal collimators placed before the monochromator, sample, and counter, and the maximum vertical divergence was 1.0°. At high temperatures, where the effect is larger, $\theta - 2\theta$ scans were employed to make absolute reflectivity measurements. For such measurements a beam area of 1.02 cm^2 was employed with no colimator in front of the counter. and the maximum vertical divergence was 0.9°. During such scans, the optimum counter position was determined, and for other temperatures the counter positions for the relative measurements were determined on the basis of the thermal expansion of silicon.[14] Our crystal thickness t_0 was 1.526 cm. The furnace

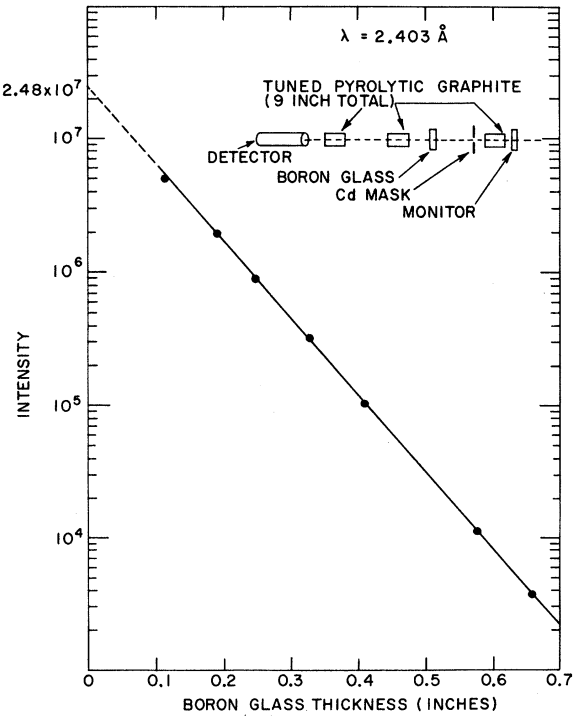

FIG. 1. Plot of the transmitted intensity vs thickness of boron-glass absorbers. Extrapolation to zero thickness determines the incident beam intensity. The arrangement of graphite filters is shown at top of the figure.

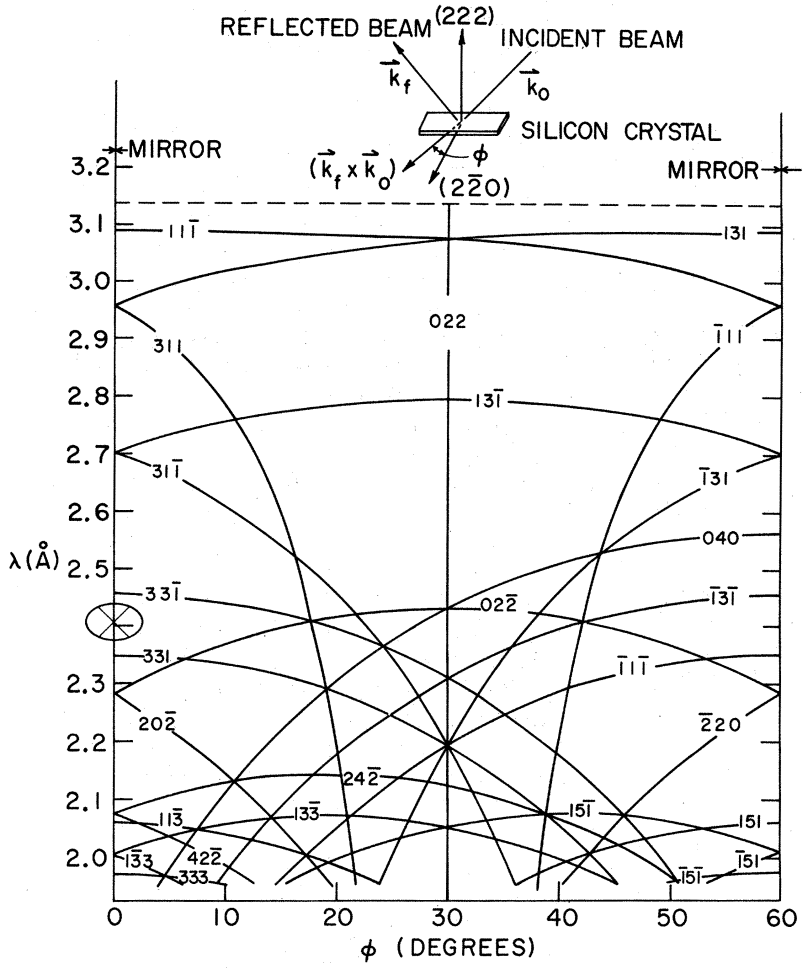

FIG. 2. Loci of double-Bragg events in which one or more reflections can occur simultaneously with the (222) reflection. The ellipse centered about $\phi = 0$ and $\lambda = 2.403$ Å is approximately the maximum extent of the resolution function. The azimuthal orientation of the crystal is defined at the top of the figure.

was a vacuum furnace capable of melting silicon with a maximum sample gradient ~ 10 °C.

We took great care to eliminate higher harmonics in our primary beam and to avoid the possibility of double-Bragg scattering. We used a germanium monochromator reflecting from the (111) planes. An additional crucial feature was the use of tuned pyrolytic graphite filters both before and after the sample to further eliminate harmonic contamination.[15] The combined length of the filters was 23 cm and their arrangement is illustrated at the top of Fig. 1. The purity of our beam was verified by the linearity of the plot in Fig. 1 of the transmitted intensity vs thickness of boron-glass absorbers over 4 orders of magnitude. Extrapolation to zero absorber thickness determined an incident beam intensity of 2.48×10^7 counts per 2×10^6 monitor count. This incident beam intensity was checked using the absolute (111) reflectivity of two perfect silicon crystals and dynamical theory to compute the primary beam intensity. These three determinations were consistent with one another to within 5%. A further check on beam purity was carried out by positioning the counter and (111) planes of the sample to diffract harmonic contaminants. None were found. At 1001 °C the purity of the (222) reflected intensity was tested with boron-glass absorbers, and no evidence of contamination was found.

The measurements of the (222) reflection were done in symmetrical Bragg geometry. The positions of double-Bragg events in which one or more reflections can occur simultaneously with the (222) reflection are readily ascertained following Cole *et al.*,[16] and are plotted in Fig. 2 as a function of azimuthal angle ϕ and wavelength λ. The azimuthal orientation of our crystal is defined in the top of the figure. We chose a wavelength $\lambda = 2.403$ Å. Our choice was predicated to eliminate both "umwegan-regung" and "aufhellung" conditions,[17] both of which are plotted in Fig. 2 (the latter corresponds to curves with even Miller indices). This choice of λ also allowed optimum tuning of the graphite filters. We chose the azimuthal position $\phi = 0$. The ellipse centered about these coordinates in Fig. 2 is approximately the maximum extent of our reso-

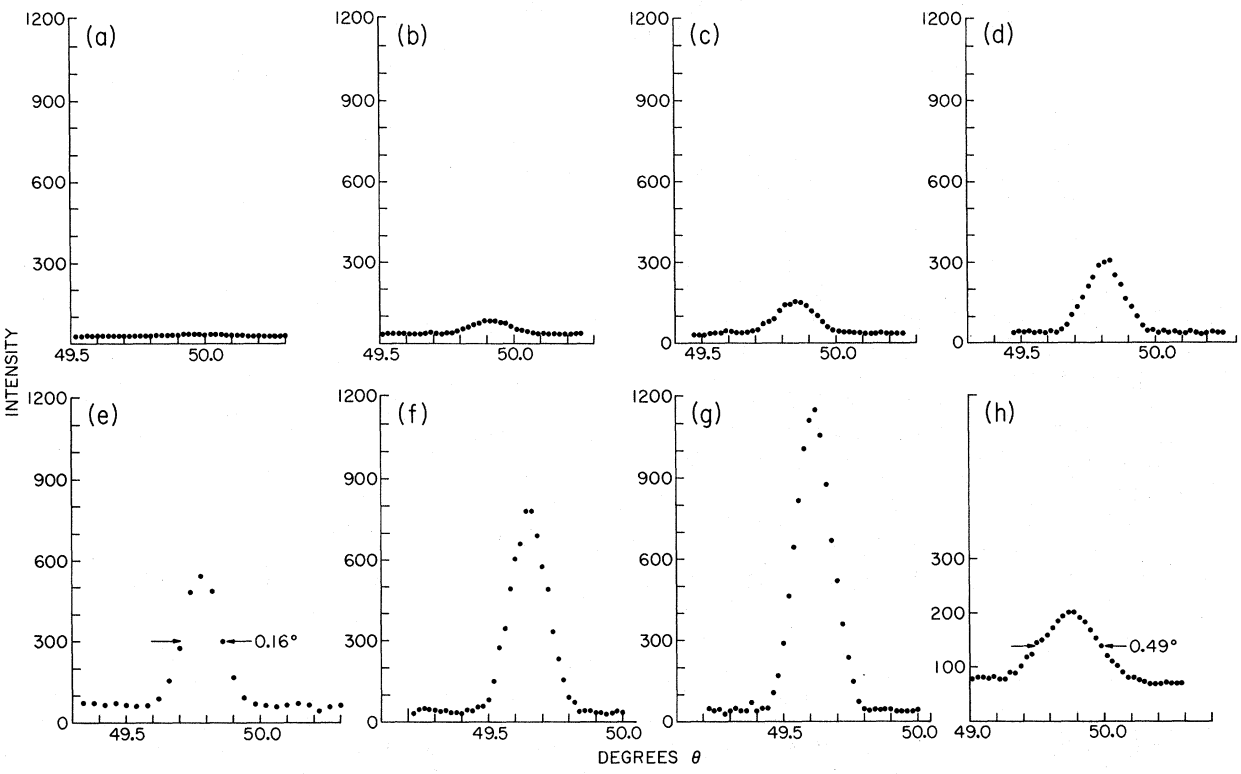

FIG. 3. θ scans through the (222) position at (a) 15, (b) 245, (c) 493, (d) 785, (e) 1001, (f) 1200, and (g) 1353 °C; (h) is a $\theta-2\theta$ scan at 1001 °C used to determine the absolute reflectivity of the (222) reflection and to normalize the θ scans. Intensities are in counts per 2×10^6 monitor count.

lution function.

The first seven peaks in Fig. 3 are θ scans through the (222) position for the temperatures indicated. The last peak in Fig. 3 is a $\theta-2\theta$ scan at 1001 °C, and was obtained with a geometry commensurate with the determination of the main beam intensity. The advantage of the geometry used in these θ scans to obtain relative values of the (222) intensity can be appreciated by comparing the θ scan at 1001 °C to the $\theta-2\theta$ scan. The over-all intensity is superior as well as the peak to background ratio. Other $\theta-2\theta$ scans (not shown) were made at 493 ° and 1353 °C. Absolute reflectivities were determined by comparing the integrated reflectivities in our $\theta-2\theta$ scans to the incident beam intensity. The relative θ scans were put in units of absolute reflectivity by normalizing the θ scan at 1001 °C to the $\theta-2\theta$ scan at 1001 °C.

In some preliminary tests, it was found that the (111) reflection decreased in intensity as the crystal temperature was raised to 500 °C. Qualitatively, this was expected from the change in the Debye-Waller factor. Upon further heating at temperatures above 500 °C, it was found that the (111) intensity increased as a function of time when the crystal was held at a constant temperature in the vicinity of 750 °C. Quantitative results made after the crystal was kept at 1001 °C showed an increase of the (111) integrated intensity by a factor of 21.5 over its initial perfect crystal value. As further measurements of the (222) were made at reduced temperatures the factor increased to 26.3 at 785 °C and 28.1 at 245 °C. The crystal was then brought to 1353 °C, our highest measuring temperature, and the factor was reduced to about 4.0; it then increased from 4.9 to 7.7 during the 1200 °C run, and finally to 9.9 when the crystal was brought to 15 °C for a final (222) measurement.

This remarkable behavior of the (111) is consistent with previous measurements of the temperature dependence of the solubility of oxygen in silicon.[18] Starting at temperatures above 500 °C, oxygen dissolved in the crystal during the growth process precipitates out in Si-O complexes. These Si-O precipitates cause considerable strain in the lattice, and for x-ray measurements[18] could completely annihilate anomalous x-ray transmission. Annealing at 1350 °C redissolves the precipitates and partially removes the strain. For the crystal used in this experiment, the ratio of the kinematic to ideally perfect (111) integrated intensity is the order of 10^3. Thus, an enhancement of the (111) by a factor of 20 due to precipitate strains is not surprising.

In converting the measured absolute (222) integrated intensity, $P(222)$, to an experimental value for $F(222)$ we used the kinematic intensity expression:

$$P(222)=N^2\lambda^3F^2(222)(1-e^{-2\mu t_0\csc\theta})/(2\mu\sin2\theta)\,, \tag{5}$$

where N is the number of cells per unit volume and t_0 is the crystal thickness. We determined an experimental linear absorption coefficient $\mu=[1170+4.35T(^\circ\mathrm{K})]\times10^{-5}\ \mathrm{cm}^{-1}$. Since our crystal is not ideally imperfect we have to justify the use of Eq. (5) to arrive at $F(222)$. For weak reflections kinematic theory should suffice because in this limit both dynamical and kinematic theories give identical results.

We can define a primary extinction coefficient, or the reflectivity of a crystal to that of an ideally imperfect crystal, as $A^{-1}\tanh(A)$ for Bragg geometry and

$$A^{-1}\sum_{n=0}^{\infty}J_{2n+1}(2A)$$

for Laue geometry.[19] The J's are Bessel functions of the first kind. For neutrons $A=|\gamma_0\gamma_1|^{-1/2}N\lambda$ $\times F(h,k,l)$, where γ_0 and γ_1 are the direction cosines describing the directions of the incident and scattered beams with respect to the crystal normal, and $|\gamma_0\gamma_1|^{-1/2}=\sin\theta$ for the Bragg case. For our (111) Laue case, $\gamma_0=0.999$ and $\gamma_1=0.743$. The quantity t is a linear dimension associated with the departure from ideal perfection, and becomes equal to the thickness of the crystal when it is ideally perfect. For large values of A as in our (111) Laue geometry the extinction coefficient becomes $(2A)^{-1}$. Thus, we may set

$$(2A)^{-1}=n[2\,|\gamma_0\gamma_1|^{1/2}N\lambda F(111)t]^{-1},$$

from which it follows that the effective thickness t is the thickness of our crystal divided by the n-fold increase in the (111) intensity. Assuming that this effective thickness is the same in all directions of the crystal, we can use the value determined from the (111) measurement to estimate the extinction coefficient for the (222) reflection. As an example, consider the worst possible case of extinction in our (222) Bragg geometry at 1353 °C for which $n=4$ and $F(2,2,2)=1.03\times10^{-14}$ cm. The extinction coefficient here is 0.850 as compared to unity for an extinction-free crystal. This would lead to an error of approximately 7% in $F(2,2,2)$. Accordingly, we have treated all our (222) data as extinction free.

In Eq. (3) we see that in the complex plane, the

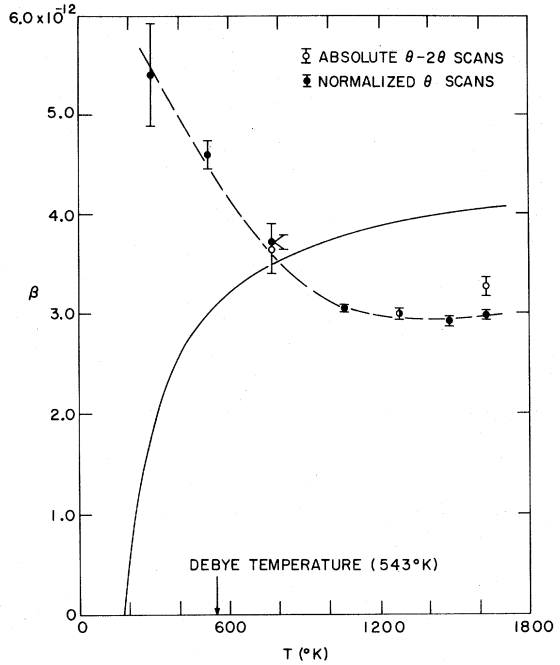

FIG. 5. Plot of the Dawson and Willis anharmonic force constant β vs T as determined from the (222) reflection, dashed line, and as determined from the thermal expansion of silicon, solid line.

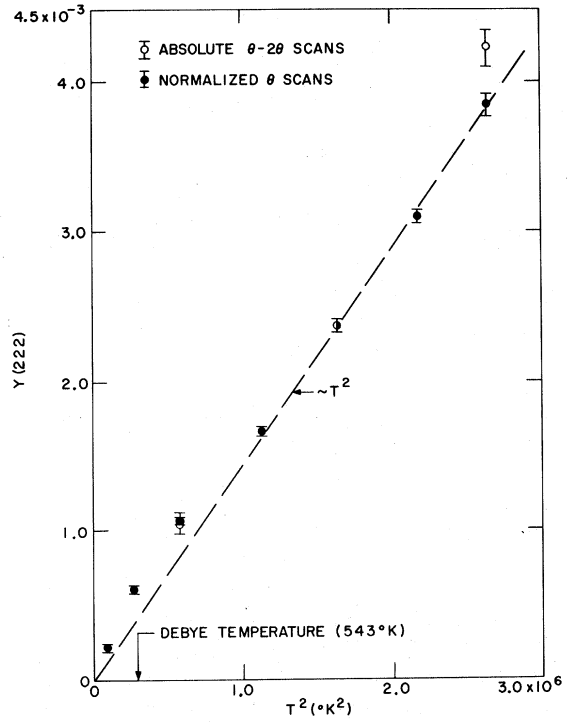

FIG. 4. Plot of $Y(2,2,2)$ vs T^2. The solid line is a line drawn through the origin $\sim T^2$. Results from three absolute $\theta-2\theta$ scans and normalized θ scans are shown.

TABLE I. Summary of neutron measurements. Values with asterisks were determined absolutely. Other values are normalized to the 1001° C absolute measurement (see text).

T (°K)	Integrated reflectivity (10^{-8} rad)	F (2, 2, 2) (10^{-14} cm)	Y (2, 2, 2) (10^{-3})	β 10^{-12} erg Å^{-3}
288	0.103 ± 0.02	0.0967 ± 0.010	0.219 ± 0.020	5.42 ± 0.54
518	0.450 ± 0.03	0.210 ± 0.006	0.602 ± 0.020	4.60 ± 0.14
766	1.15 ± 0.04	0.339 ± 0.006	1.06 ± 0.02	3.72 ± 0.07
	*1.07 ± 0.10	*0.334 ± 0.015	*1.05 ± 0.05	*3.65 ± 0.16
1058	2.40 ± 0.06	0.496 ± 0.007	1.67 ± 0.02	3.05 ± 0.04
1274	4.37 ± 0.18	0.675 ± 0.014	2.37 ± 0.05	2.99 ± 0.06
	*4.37 ± 0.09	*0.675 ± 0.007	*2.37 ± 0.02	*2.99 ± 0.03
1473	6.85 ± 0.20	0.852 ± 0.010	3.10 ± 0.04	2.92 ± 0.04
1626	9.92 ± 0.17	1.03 ± 0.02	3.85 ± 0.06	2.98 ± 0.05
	*11.8 ± 0.7	*1.13 ± 0.03	*4.24 ± 0.13	*3.29 ± 0.10

structure factor $F(2, 2, 2)$ is represented by the sum of two vectors separated by an angle γ. Writing

$$F^2(2, 2, 2) = V_\alpha^2 + V_\beta^2 + 2V_\alpha V_\beta \cos\gamma ,$$

we may solve for V_β:

$$V_\beta = -V_\alpha \cos\gamma + [F^2(2, 2, 2) - V_\alpha^2 \sin^2\gamma]^{1/2}, \qquad (6)$$

where

$$V_\alpha = 8e^{-M} f_b (C_s^2 + C_f^2)^{1/2} ,$$

$$V_\beta = 8e^{-M} [C_s^2 (Z - f_c)^2 \cot^2\theta + (b + C_f f_c)^2]^{1/2} Y(h, k, l)$$

and

$$\tan\gamma = \frac{-(b + C_f f_c)(Z - f_c)^{-1} - C_f}{C_s \cot\theta - C_f (b + C_f f_c)^{-1} C_s (Z - f_c)^{-1} \tan\theta} .$$

From the experimental $F(222)$ and Eq. (6), we then found the quantity $Y(2, 2, 2)$ which is plotted as a function of T^2 in Fig. 4. Both the results from the normalized θ scans and the three absolute $\theta - 2\theta$ scans are shown. If extinction were present to any large degree at 1353 °C, we should not expect these points to lie on or above the line drawn proportional to T^2 in Fig. 4. In Fig. 5, β is plotted as a function of T. The solid curve in Fig. 5 is the value of β derived from the thermal expansion of silicon.[14] The two methods of arriving at a value of β are in close agreement at high temperature and tend toward a constant value. However, at lower temperatures the two methods give values of β which diverge from a constant value in opposite ways. This is not unexpected from the failure of the overly simplified Einstein model to properly account for the true frequency spectrum of a solid. Table I is a summary of the results of the neutron measurements.

The quantity $Y(2, 2, 2)$ is precisely the quantity needed to sort from the x-ray structure factor that part arising from the anticentrosymmetric charge density from that due to the anharmonic thermal motion. We are able to write then

$$f_b e^{-M} = F_{\text{x ray}}(2, 2, 2)/8i + f_c e^{-M} Y(h, k, l). \qquad (7)$$

Figure 6 is a plot of $f_b e^{-M}$ vs T'. $T' = [\Phi(X) + \frac{1}{4}X]$, where the quantity in the bracket is the Debye function.[20] Here $X = \Theta/T$, and Θ is the Debye temperature of silicon,[21] 543.°K. T' is ~ 8% greater than T at room temperature and ~ 1% greater than T at 1353 °C. We have used the variation with

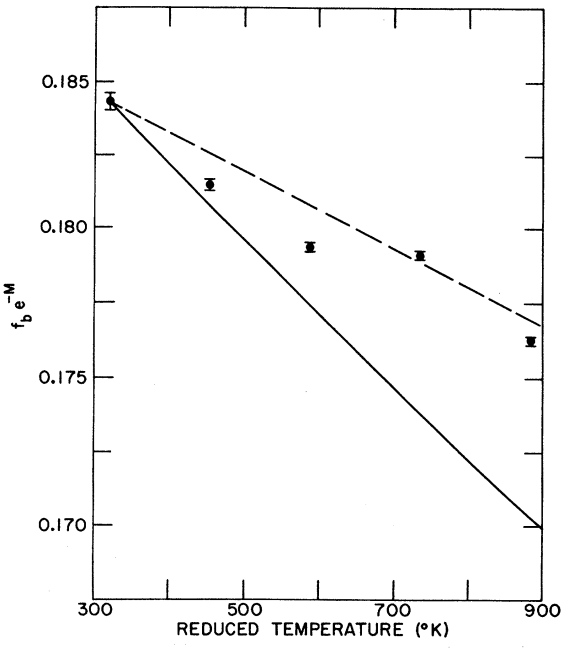

FIG. 6. Scattering from the bonding charge density, $f_b e^{-M}$, vs T'. The solid line is the expected variation on the basis of the rigid ion model, i.e., $\sim e^{-M}$. The dashed line indicates the variation expected if the bonding electrons vibrated with half the mean-square amplitude of the core, i.e., $\sim e^{-M/2}$.

temperature of $F_{x\ ray}$ (2, 2, 2) previously determined.[3] The solid line in Fig. 6 is the expected temperature dependence due to the Debye-Waller factor predicted on the basis of the rigid ion model.[22,23] The dashed line, given merely as a reference, indicates the expected temperature dependence of $f_b e^{-M}$ if the bond electrons vibrated with half the mean square amplitude of the core.

The rigid ion model assumes an electron charge density rigidly attached to the atomic nucleus which is incapable of distorting as the ions are displaced. We take Fig. 6 as conclusive evidence of the failure of the rigid ion model, for the scattering due to the bonding electrons in Fig. 6 is clearly less temperature dependent than that from the core. We view this bonding charge density as moving with less thermal amplitude than the nucleus or core charge density. In fact, this supports in a direct way the concepts of the shell model.[24]

III. DISCUSSION

We attribute the temperature variation of β in Fig. 5 as derived from either the thermal expansion or our (222) data to the inadequacy of the Einstein model. We expect that a near-neighbor anharmonic potential will suffice to explain our results when the phonon occupation numbers and frequency distribution of silicon are adequately accounted for. Our $Y(h,k,l)$ is related to the anharmonic Debye-Waller factor discussed by Cowley[23] and others. In particular, it is proportional to his diagram (b) which is usually overlooked because it does not contribute to the Debye-Waller factor in a Bravais lattice.[23,25] However, such an expression does contribute in a diamond structure. The high-temperature limit of this expression contains a term linear in T as well as T^2. A term in T cannot be deduced from the Einstein model. Such a term qualitatively accounts for the lower-temperature behavior seen in Fig. 4. Computer calculations incorporating these ideas are in progress. However, the purpose and scope of this experiment are adequately served by concepts introduced by Dawson and Willis.

ACKNOWLEDGMENTS

The authors wish to thank G. H. Schwuttke of the IBM Laboratory, Poughkeepsie, New York for supplying us with a large single crystal of silicon from which our crystals were cut. We wish also to express our indebtedness to Julius Hastings for the use of a chemistry neutron diffractometer and to Gen Shirane for extra pyrolytic graphite filters.

---

†Work supported by the U.S. Atomic Energy Commission.

[1]L. Pauling, *The Nature of the Chemical Bond* (Cornell U. P., Ithaca, New York, 1960), p. 116.

[2]W. H. Bragg, Proc. Phys. Soc. (London) 33, 304 (1921).

[3]J. B. Roberto and B. W. Batterman, Phys. Rev. B 2, 3220 (1970).

[4]B. Dawson and B. T. M. Willis, Proc. Roy. Soc. (London) A298, 307 (1966).

[5]L. L. Foldy, Phys. Rev. 87, 693 (1952); Rev. Mod. Phys. 30, 471 (1958).

[6]V. E. Krohn and G. R. Ringo, Phys. Rev. 148, 1303 (1966).

[7]J. Schwinger, Phys. Rev. 73, 407 (1948).

[8]G. Obermair, Z. Physik 204, 215 (1967).

[9]*International Tables for X-Ray Crystallography*, edited by C. H. MacGillavry, G. D. Rieck, and K. Lonsdale (Kynock Press, Birmingham, 1962), Vol. III, p. 122.

[10]See Reference 9, Vol. III, p. 202.

[11]C. G. Shull, Phys. Rev. Letters 21, 1585 (1968) (corrected, 1971, Shull, private communication).

[12]R. Colella and A. Merlini, Phys. Status Solidi 18, 157 (1966).

[13]A. C. Nunes, Acta Cryst. A27, 219 (1971).

[14]*Handbook of Thermophysical Properties of Solid Materials*, edited by A. Goldsmith, T. E. Waterman, and H. J. Hirschhorn (Macmillan, New York, 1967), Vol. 1, p. 581.

[15]G. Shirane and V. J. Minkiewicz. Nucl. Instr. Methods 79, 109 (1970).

[16]H. Cole, F. Chambers, and H. Dunn, Acta Cryst. 15, 138 (1962).

[17]R. M. Moon and C. G. Shull, Acta Cryst. 17, 805 (1964).

[18]J. R. Patel and B. W. Batterman, J. Appl. Phys. 34, 2716 (1963).

[19]W. H. Zachariasen, *Theory of X-Ray Diffraction in Crystals* (Oxford U. P., Oxford, England, 1954), pp. 133 and 134.

[20]See Ref. 9, Vol. III, p. 233.

[21]B. W. Batterman and D. R. Chipman, Phys. Rev. 127, 690 (1962).

[22]M. Born and K. Huang, *Dynamical Theory of Crystal Lattices*, (Oxford U. P., Oxford, England, 1954).

[23]R. A. Cowley, Advan. Phys. 12, 421 (1965).

[24]W. Cochran, Proc. Roy. Soc. (London) 253, 260 (1959).

[25]A. A. Maradudin and A. E. Fein, Phys. Rev. 128, 2589 (1962).